BIOCHEMISTRY
including biophysical chemistry & molecular biology

Article

pubs.acs.org/biochemistry

Allosteric Interaction of Nucleotides and tRNA^{ala} with *E. coli* Alanyl-tRNA Synthetase

John David Dignam,*[,†] Jingshu Guo,[‡] Wendell P. Griffith,[‡] Nichola C. Garbett,[§] Amanda Holloway,[†] and Timothy Mueser[‡]

[†]Department of Biochemistry and Cancer Biology, University of Toledo College of Medicine, 3035 Arlington Ave. Toledo, Ohio 43614, United States

[‡]Department of Chemistry, University of Toledo, M.S. 602, 2801 W. Bancroft St., Toledo, Ohio 43606, United States

[§]James Graham Brown Cancer Center, University of Louisville, Clinical and Translational Research Building, 505 S. Hancock St., Louisville, Kentucky 40202, United States

Supporting Information

ABSTRACT: Alanyl-tRNA synthetase, a dimeric class 2 aminoacyl-tRNA synthetase, activates glycine and serine at significant rates. An editing activity hydrolyzes Gly-tRNA^{ala} and Ser-tRNA^{ala} to ensure fidelity of aminoacylation. Analytical ultracentrifugation demonstrates that the enzyme is predominately a dimer in solution. ATP binding to full length enzyme (ARS875) and to an N-terminal construct (ARS461) is endothermic (ΔH = 3−4 kcal mol^{-1}) with stoichiometries of 1:1 for ARS461 and 2:1 for full-length dimer. Binding of aminoacyl-adenylate analogues, 5′-*O*-[*N*-(L-alanyl)sulfamoyl]-adenosine (ASAd) and 5′-*O*-[*N*-(L-glycinyl)sulfamoyl]-adenosine (GSAd), are exothermic; ASAd exhibits a large negative heat capacity change (ΔC_p = 0.48 kcal mol^{-1} K^{-1}). Modification of alanyl-tRNA synthetase with periodate-oxidized tRNA^{ala} (otRNA^{ala}) generates multiple, covalent, enzyme−tRNA^{ala} products. The distribution of these products is altered by ATP, ATP and alanine, and aminoacyl-adenylate analogues (ASAd and GSAd). Alanyl-tRNA synthetase was modified with otRNA^{ala}, and tRNA-peptides from tryptic digests were purified by ion exchange chromatography. Six peptides linked through a cyclic dehydromorpholino structure at the 3′-end of tRNA^{ala} were sequenced by mass spectrometry. One site lies in the N-terminal adenylate synthesis domain (residue 74), two lie in the opening to the editing site (residues 526 and 585), and three (residues 637, 639, and 648) lie on the back side of the editing domain. At least one additional modification site was inferred from analysis of modification of ARS461. The location of the sites modified by otRNA^{ala} suggests that there are multiple modes of interaction of tRNA^{ala} with the enzyme, whose distribution is influenced by occupation of the ATP binding site.

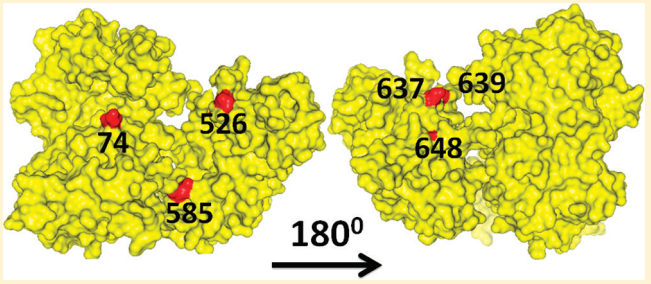

Aminoacyl-tRNA synthetases attach amino acids to their cognate tRNAs in protein biosynthesis[1−9] through an aminoacyl-adenylate intermediate. Analysis of the thermodynamics, dynamics, and kinetics of coupled ligand interaction with these enzymes is essential to understanding their catalytic mechanisms. The principle of cooperativity and ligand-induced fit[10] is a recurring theme in enzymology and is amply illustrated in structural and kinetic studies of class 1 and class 2 aminoacyl-tRNA synthetases. Examples of tRNA binding-induced conformational transitions affecting aminoacyl-adenylate synthesis are seen in arginyl-,[11−14] glutamyl-,[15−18] glutaminyl-tRNA synthetases[19−22] and class 1 lysyl-tRNA synthetase which require tRNA for this step. Structural[23] and pre-steady-state kinetic studies of glutaminyl-tRNA synthetase[21] indicate that interactions between the tRNA anticodon and the enzyme result in changes in the positions of distal active site elements that interact with glutamine and ATP. In seryl-tRNA synthetase, tRNA binding results in a switch in some residues from interaction with ATP or the aminoacyl-adenylate to interaction with tRNA.[24] With yeast seryl-tRNA synthetase, tRNA binding increases the specificity and efficiency of adenylate formation[25,26] and suppresses misactivation of threonine. Threonyl-,[27−29] aspartyl-,[30−33] and prolyl-tRNA synthetases[34] exhibit conformational transitions induced by tRNA, ATP, and their cognate amino acids. These studies imply that binding of the amino acid, ATP, and tRNA is linked, structurally and thermodynamically, to promote catalysis and to ensure specificity of tRNA and amino acid recognition.

E. coli alanyl-tRNA synthetase is a dimeric, class 2a enzyme[35,36] of identical 875 residue, 96 000 molecular weight subunits[37,38] with three functional elements. The N-terminal domain synthesizes alanine-adenylate as an intermediate for tRNA aminoacylation.[39−42] A zinc-dependent hydrolase

Received: August 2, 2011
Revised: September 13, 2011
Published: October 10, 2011

domain recognizes and edits misacylated tRNA^{ala}, deacylating Gly-tRNA^{ala}, and Ser-tRNA^{ala}, but not Gly-tRNA^{thr}.[43] This structure recognizes misacylated tRNA^{ala} in the absence of the adenylate synthesis domains, implying that the enzyme has separate tRNA^{ala} recognition sites, one for uncharged tRNA^{ala} and a second for misacylated tRNA^{ala} (Ser-tRNA^{ala} and Gly-tRNA^{ala}). There is evidence for pretransfer editing that selectively eliminates incorrect adenylates;[43,44] pretransfer editing activities are seen in a number of tRNA synthetases.[45−52] A C-terminal coiled-coil plus globular element mediates dimer formation[53] and plays a role in tRNA binding and editing.[54] Although no structure is available for the entire protein from any species, a model was proposed based on structures of the aminoacylation-editing domains and the dimeric coiled-coil globular domain of the *Archeoglobus fulgidus* alanyl-tRNA synthetase.[53] There are structures for the aminoacylation-editing domains from *Pyrococcus horikoshii*,[55] the N-terminal aminoacylation domains from *Aquifex aeolicus*[56,57] and *E. coli*,[58] and a free-standing editing protein from *Pyrococcus horikoshii*.[59,60] The N-terminal catalytic domain of *E. coli* alanyl-tRNA synthetase[61] was crystallized after introduction of a leucine half zipper into an exposed α-helix.[58] Structures of the *E. coli* enzyme are of interest insofar as most of the mutational analysis on this enzyme and its cognate tRNA were performed on this protein.

There are no structures of complexes of alanyl-tRNA synthetase with tRNA^{ala}. Two models have been proposed for the interaction of the protein with tRNA, one based on part of the structure of the *A. aeolicus* enzyme[57] and the other on the structure of the aminoacylation-editing domains of the *A. fulgidus* enzyme.[53] Neither model addresses how tRNA^{ala} interacts with the editing domain or the C-terminal globular domain. To identify protein−tRNA contacts in different alanyl-tRNA synthetase-tRNA^{ala} ligand complexes, we employed affinity labeling to identify lysyl residues in proximity to the 3′-end of tRNA^{ala} bound to alanyl-tRNA synthetase. Incubation of alanyl-tRNA synthetase with tRNA^{ala} with the ribose of adenosine 76 oxidized to a dialdehyde (otRNA^{ala}) results in multiple modified species whose relative abundance changes in the presence of ATP, alanine, ATP and alanine, (5′-*O*-[*N*-(L-alanyl)sulfamoyl]adenosine (ASAd), and a noncognate adenylate analogue, 5′-*O*-[*N*-(L-glycinyl)sulfamoyl]adenosine (GSAd). We identified six lysyl residues: one near the adenylate-synthesis site (lys 74) and five in the editing domain (lys 526, 585, 637, 639, and 648). The data indicate that ligands alter the interaction of the 3′-end of tRNA^{ala} with the enzyme, resulting in reaction of the 3′-dialdehyde with different sites on the protein. The results confirm work identifying lys74 in the adenylate synthesis domain[62] as a modification site and identify five modification sites in the editing domain, consistent with models proposed earlier[63,64] which have the 3′-end of the nonacylated tRNA residing in the editing site. During this work we reexamined the oligomeric state of alanyl-tRNA synthetase, confirming earlier studies indicating that it is predominately a dimer in solution[37,38] and not a tetramer.[65]

EXPERIMENTAL PROCEDURES

Materials. Modified, sequencing grade trypsin was from Boehringer Ingelheim (Ridgefield, CT). 5′-*O*-[*N*-(L-Alanyl)-sulfamoyl]adenosine and 5′-*O*-[*N*-(L-glycinyl)sulfamoyl]-adenosine were obtained from Integrated DNA Technologies (Coralville, IA). Superose 12 and MonoQ HPLC columns, Sephacryl S200, Q-Sepharose, and Sephadex G50 (medium) were from GE Healthcare (Waukesha, WS).

Analytical Procedures. SDS polyacrylamide gel electrophoresis of protein samples was performed as previously described.[66] RNA samples were subjected to electrophoresis denaturing conditions on 12% acrylamide gels in the presence of 8 M urea, 0.089 M Tris-borate buffer, and 2 mM EDTA. Aminoacyl-tRNA synthetase assays are described in refs 67 and 68 in 20 mM Hepes NaOH (pH 7.5), 100 mM KCl, 5 mM $MgCl_2$, 0.2 mM EDTA, 0.1 mg mL^{-1} acetylated bovine serum albumin, 0.2 mM alanine (^{14}C labeled), and 8 μM tRNA^{ala}.

Inhibition of Alanyl-tRNA Synthetase by ASAd and GSAd. The effects of ASAd and GSAd as inhibitors of alanyl-tRNA synthetase were analyzed assuming that these compounds act as geometric inhibitors with respect to ATP and the amino acid.[69] Inhibition constants were calculated from the relationship

$$v = (V[\mathrm{ATP}][\mathrm{ala}])/([\mathrm{ATP}][\mathrm{ala}] + K_{\mathrm{ATP}}[\mathrm{ala}] + K_{\mathrm{ala}}[\mathrm{ATP}] + K_{i\mathrm{ATP}}K_{\mathrm{ala}}(1 + [\mathrm{I}]/K_i))$$

In this expression K_{ala} (340 μM) and K_{ATP} (95 μM) are the Michaelis constants for alanine and ATP, respectively, K_{iATP} is the dissociation constant for ATP binding to free enzyme (15 μM) based on ITC experiments, [I] is the concentration of the inhibitor (ASAd or GSAd), and K_i is the dissociation constant of the inhibitor.

Isothermal Titration Calorimetry. Isothermal titration calorimetry (ITC) was performed with a Microcal VPITC.[70] Protein samples were prepared for titrations by chromatography on Sephadex G50 medium equilibrated in 20 mM Hepes NaOH (pH 7.5), 100 mM KCl, 5 mM $MgCl_2$, and 0.2 mM EDTA to exchange the solvent, degassed, and used immediately. ATP solutions were prepared as Mg·ATP in the same buffer with 5 mM free Mg^{2+}. Titrations were performed at 25 °C, at a stir rate of 310 rpm, with ligand injected at 0.5 μL/s, with 300 s between injections. Protein concentrations, syringe ligand concentrations, and injection volumes are indicated in figure legends. Blank titrations of ligand into buffer to determine the heat of dilution consisted of the same number of solution injections as the titrations into enzyme solutions. Binding data were analyzed assuming a single class of binding sites using Origin v7.0 (OriginLab Corp., Northampton, MA) software provided with the instrument.

Purification of *E. coli* Alanyl-tRNA Synthetase. Expression vectors were constructed by inserting PCR amplified products encoding full length *E. coli* alanyl-tRNA synthetase (ARS875) or the N-terminal 461 residues (ARS461) between the Nde I and *Sal*I sites of plasmid pET12a. The sequence of the insert was verified, and the plasmids were transformed into BL21DE3star. Cells were grown at 37 °C in LB/M9 and induced with 0.2 mM IPTG when the cultures reached an A_{600} of 0.5−0.8. Cells were grown for 4−5 h after induction, collected by centrifugation, washed once with 0.15 M NaCl, and stored as cell pellets at −80 °C. Purification was conducted at 0−4 °C, except as indicated for chromatography on Superose 12. Cells were suspended in six volumes of 50 mM Tris-HCl (pH 7.5 at 25 °C), 10% v/v glycerol, 0.1% v/v Triton X-100, 2 mM EDTA, 1 mM DTT, 1 mM PMSF, 10 μg mL^{-1} leupeptin, and 50 μg mL^{-1} hen egg white lysozyme. The suspension was homogenized with a Dounce homogenizer to reduce the viscosity. ATP was added to 5 mM, and $MgCl_2$ was added to 10 mM. The suspension was centrifuged for 60 min in

a GS3 rotor (Beckman) at 7000 rpm, and the supernatant fraction was retained. For ARS875, 0.25 volumes of 50% (w/v) poly(ethylene glycol) 6000 (50 mM Tris-HCl (pH 7.5 at 25 °C)) was added to the supernatant with stirring. After 30 min the suspension was centrifuged for 30 min in a GS3 rotor (Beckman) at 7000 rpm, and the precipitate was dissolved in 20 mM Tris-HCl (pH 7.8 at 25 °C), 10% v/v glycerol, 0.2 mM EDTA, and 0.5 mM DTT (buffer B) for chromatography on Q-Sepharose. For ARS461, 0.2 volumes of 50% (w/v) poly-(ethylene glycol) 6000 was added to the extract and stirred for 30 min followed by centrifugation. $MgCl_2$ was added to the supernatant to 12 mM (22 mM final $MgCl_2$) followed by 0.47 volumes (relative to the original extract) of 50% (w/v) poly(ethylene glycol) 6000. The material was stirred for 30 min and centrifuged to recover the precipitate, and the precipitate was dissolved in buffer B for chromatography on Q-Sepharose. Fractions from PEG precipitation were applied to Q-Sepharose (1.4 mL of resin per gram of bacterial pellet) equilibrated in buffer B. The column was washed with one column volume of buffer B and eluted with a 10 column volume linear gradient from 0 to 0.25 M Na_2SO_4. ARS875 eluted at ∼0.1 M Na_2SO_4 and ARS461 eluted at ∼0.05 M Na_2SO_4. Based on assays of enzyme activity and the results of SDS gel electrophoresis, fractions were pooled and concentrated to a small volume using an Amicon ultrafiltration cell with a PM10 membrane. For large scale preparations the material was applied to Sephacryl S200 (2.5 cm × 84 cm) equilibrated in 50 mM potassium phosphate (pH 7.0), 10% v/v glycerol, 0.2 mM EDTA, and 0.5 mM DTT; the column was eluted at 4 °C. For smaller scale preparations the material was applied to Superose 12 equilibrated in the same buffer as Sephacryl S200 but run at room temperature. Fractions were analyzed by SDS gel electrophoresis, pooled, concentrated by ultrafiltration, and stored as small aliquots at −70 °C.

Analytical Gel Filtration. Gel filtration to obtain size estimates was performed using Superose 12 equilibrated in 20 mM Hepes-NaOH (pH 7.5 at 25 °C), 100 mM KCl, 5 mM $MgCl_2$, 0.2 mM EDTA, and 1 mM TCEP. Samples of 0.5 mL at 1 mg mL^{-1} were injected and eluted at 0.5 mL min^{-1} at 22 °C. Thyroglobulin, immunoglobulin G, human serum albumin, ovalbumin, and bovine myoglobin were employed as standards using the same conditions for chromatography.

Analytical Ultracentrifugation. Analytical ultracentrifugation was performed at the Biophysical Core Facility at the University of Louisville. Samples of alanyl-tRNA synthetase were prepared for analytical ultracentrifugation experiments by exchanging the buffer on a column of Sephadex G50 equilibrated in 20 mM Hepes-NaOH (pH 7.5 at 25 °C), 100 mM KCl, 5 mM $MgCl_2$, 0.2 mM EDTA, and 1 mM tris(2-carboxyethyl)phosphine HCl. The calculated subunit molecular weight (without the N-terminal methionine) is 95 898. Sedimentation velocity (SV) and sedimentation equilibrium (SE) experiments were performed at 20 °C using a Beckman Optima XL-A analytical ultracentrifuge equipped with absorbance optics and an An60Ti rotor (Beckman Coulter, Inc., Palo Alto, CA). Data were collected at 280 nm as a function of radial position at three loading concentrations of A_{280} ∼ 0.2, 0.5, and 1.0. SV and SE analyses were performed over a 4-fold loading concentration range to examine the effects of increasing sample concentration; for the wild-type enzyme (ARS875) the extinction coefficient for a 1 mg mL^{-1} solution was taken as 0.72.[38] Solution density and viscosity were calculated at 20 °C from buffer composition as 1.007 24 g mL^{-1} and 1.0173 cP, respectively, using the program Sednterp.[71] The partial specific volume was calculated at 20 °C as 0.7321 mL g^{-1} from the amino acid sequence using Sednterp. SV experiments were performed at a rotor speed of 50 000 rpm. Before data collection, samples were allowed to equilibrate for 1 h after vacuum and temperature had been established. Each centrifuge cell was scanned sequentially with zero time delay between scans until no further sedimentation was observed as judged by monitoring the standard deviation between successive scans using WinMatch.[72] Primary SV data were transferred to the program Sedfit and Sedanal for analysis.[73−77] Data were analyzed with Sedfit using a continuous $c(s)$ model with a range of 0.5−12 S and a confidence level of 0.68 (1 standard deviation). Fitting was performed using alternating rounds of the simplex and Marquardt−Levenberg algorithms until there was no further decrease in rmsd. Data analyzed with DCDT+ were subjected to transformation into a differential apparent sedimentation coefficient distribution, $g(s^*)$, and evaluating with and without recourse to model fitting. Distributions in the form of $c(s)$ and $g(s^*)$ were plotted using Origin v7.0 (OriginLab Corp., Northampton, MA). Sedimentation equilibrium (SE) experiments were performed at rotor speeds of 8000, 10 000, and 12 000 rpm, followed by the determination of y_{offset} values from the residual absorbance measured at 40 000 rpm. Samples of A_{280} ∼ 0.2, 0.5, and 1.0 were loaded into six-channel cells with the reference sectors filled with matched buffer. Scans were collected every 30 min until equilibrium was attained as judged by monitoring the standard deviation between successive scans using WinMatch. Primary SE data were cast into the form of the natural logarithm of the equilibrium sample concentration as a function of radial position as $\ln(c)$ vs $r^2/2$, following correction for an experimentally determined y_{offset} value, and graphed using Origin v7.0. SedAnal v5.03[78] and Beckman Coulter Optima XL-A/XL-I Data Analysis software v6.03 were used for additional model fitting and global analysis of both SV and SE data.

Purification of $tRNA^{ala}$. $tRNA^{ala}$ was expressed from plasmid p-EctRNA^{ala} which has the $tRNA^{ala}$ (GGC anticodon) sequence inserted into pEXT20 (provided by Paul Schimmel, Scripps Research Institute). The $tRNA^{ala}$ was expressed in MRE600 grown in 2X LB with 100 μg mL^{-1} ampicillin at 37 °C, induced with IPTG (0.2 mM), and grown for 15 h after induction. Cells were harvested, suspended in 5 volumes of 0.1 M NaAcetate (pH 4.5) and 1 mM EDTA, extracted twice for 30 min with an equal volume of water-saturated phenol and once with an equal volume of chloroform, and precipitated with 2.5 volumes of ethanol. The tRNA was subjected to chromatography on benzolyated DEAE cellulose.[79] Active fractions were identified by aminoacylation with ^{14}C alanine and subjected to chromatography on phenyl Sepharose (60 mL bed volume); the column was equilibrated in 50 mM NaAcetate (pH 5.2), 1.7 M $(NH_4)_2SO_4$, and 10 mM $MgSO_4$ and eluted with an eight column volume linear gradient from 1.7 to 1.1 M $(NH_4)_2SO_4$. Fractions were pooled based on acceptor activity and dialyzed against 50 mM NaAcetate (pH 4.5), 250 mM NaCl and 10 mM $MgCl_2$ followed by precipitation with ethanol. The tRNA was dissolved in sterile 5 mM $MgCl_2$ and stored at −20 °C. Acceptor activity was 46 nmol per mg of RNA. The purified tRNA gave a single band on denaturing gel electrophoresis in 8 M urea.

Preparation of Periodate Oxidized tRNA. tRNA at 10 mg mL^{-1} was incubated in 0.1 M NaAcetate (pH 4.5) and 10

mM $NaIO_4$ for 10 min on ice. The RNA was precipitated with 2.5 volumes of ethanol, and the precipitate was collected by centrifugation and dried. The resulting otRNA^{ala} was dissolved in an appropriate volume of sterile water and used immediately.

Modification of Alanyl-tRNA Synthetase with otRNA^{ala}. Alanyl-tRNA synthetase (at 2 mg mL^{-1}) was incubated in 20 mM MOPS-NaOH (pH 7.3), 100 mM KCl, 5 mM $MgCl_2$, 1 mM DTT, and 10 mM $NaCNBH_3$ with 75 μM otRNA^{ala} at 30 °C. Other ligands (e.g., ATP, alanine, AMP) were added as indicated for specific experiments. Time of incubation is indicated for specific experiments. For the isolation of tRNA peptides, alanyl-tRNA synthetase (at 3.6 mg mL^{-1}) was incubated for 3 h in a 1 mL reaction as indicated above in the presence of 5 mM Mg·ATP. The reaction mixture was applied to Superose 12 equilibrated in 0.1 M NH_4HCO_3 and 10 mM $MgCl_2$ to resolve residual otRNA^{ala} from the modified enzyme. Fractions were analyzed by SDS gel acrylamide electrophoresis, and fractions containing modified enzyme were pooled for further analysis.

Trypsin Digestion of otRNA^{ala}-Modified Alanyl-tRNA Synthetase and Isolation of tRNA Peptides. Fractions from Superose 12 containing otRNA^{ala}-modified alanyl-tRNA synthetase (3.5 mg) were precipitated with 3 volumes of ethanol, dried, suspended in 1.25 mL of 20 mM Tris-HCl (pH 8.0), 100 mM NaCl, and 10 mM $MgCl_2$, and digested with 25 μg of modified trypsin at 30 °C for 17 h. The digest was precipitated with 2.5 volumes of 95% ethanol. The resulting precipitate was dissolved in water and adjusted to 20 mM sodium acetate (pH 4.5) and 5 mM $MgCl_2$ in 4 mL. The material was applied to a 1.1 mL bed volume Mono Q column (GE Healthcare) equilibrated in the same solvent. The column was eluted at 0.5 mL/min. The tRNA peptides were eluted with a gradient from 0 to 0.5 M NaCl over 20 min and 0.5 to 1 M NaCl over 5 min. Fractions containing 260 nm absorbing material (tRNA-peptides) were analyzed by gel electrophoresis and pooled. The tRNA-peptides were adjusted to pH 7.5 with MOPS (0.1 M) in 1.6 mL and incubated with boiled pancreatic ribonuclease A (6 μg mL^{-1}) for 2 h at 37 °C. A sample of purified tRNA^{ala} (0.5 mg) was digested with RNAase A under the same conditions in parallel with the tRNA peptides for use as a control on the HPLC.

Purification of Peptides by Reversed Phase Chromatography. HPLC reversed phase chromatography was performed on a Shimadzu Biotech Prominence HPLC (Columbia, MD). Peptides derived from the digestion of the otRNA^{ala}-modified alanyl-tRNA synthetase were dissolved in 0.1% TFA and applied to a 4.6 × 100 mm BDS Hypersil C18 (3 μm particle size) (Thermo Electron Corp., Marietta, OH). Elution solvent A was 0.1% TFA in water, and solvent B was 0.1% TFA in acetonitrile (ACN). Gradient elution at a flow rate of 0.5 mL/min was carried out as follows: isocratic at 15% B for 10 min, increased to 60% B over 80 min, and then increased to 95% B over 10 min. Absorbance was monitored at 214 and 260 nm. Fractions of 0.5 mL were collected and dried for analysis by mass spectrometry. Oxidized methionines detected in the sequence were likely generated during peptide isolation and not during modification with otRNA^{ala}; they are frequently found in the MS analysis of proteins and peptides.

Mass Spectrometry. Fractions were reconstituted in 0.1% formic acid, 50% ACN in water. MS analyses of the HPLC fractions were performed on a Synapt HDMS quadrupole time-of-flight mass spectrometer equipped with a nanoESI source (Waters, Milford, MA) and operated in the positive ionization mode. Instrument parameters for MS1 were maintained at the following values for each experiment: capillary voltage, 3.5 kV; source temperature, 80 °C; desolvation temperature, 150 °C; sample cone, 40 eV; cone gas flow rate, 0 L/h; trap collision energy, 6 eV; transfer collision energy, 4 eV. Trap collision energy was increased to between 20 and 35 eV during MS/MS for fragmentation of parent ions. Mass spectra were collected in the mass range 50−3000 m/z, which was calibrated using a solution of cesium iodide. Mass spectra were collected at a scan rate of 1 s^{-1}. Five minutes of scans were averaged for each data set, and each mass spectrum was transformed using MaxENT3 software to facilitate data analysis by converting all multiply charged fragment ions in the mass spectra to their corresponding singly charged species. Fragment ion m/z values (monoisotopic) expected for unmodified and modified peptides were calculated using the MS-product function of Protein Prospector.

The sequence of the editing domain of *E. coli* alanyl-tRNA synthetase was aligned with the sequence of the editing domain of the *A. fulgidus* protein, modeled on this structure using Swissmodel and subjected to energy minimization. This modeled structure and the structure of the adenylate synthesis domain with bound alanine sulfamoyl adenosine were superimposed on the structure of the adenylate synthesis-editing domains of the *A. fulgidus* protein as a complex with alanine sulfamoyl adenosine. Figures were rendered using PyMol version 1.3 [DeLano, W. L. The PyMOL Molecular Graphics System (2002) DeLano Scientific, San Carlos, CA]. The structure of tRNA was docked on the model of alanyl-tRNA synthetase manually using PyMOL.

RESULTS

Oligomeric State of Alanyl-tRNA Synthetase. Alanyl-tRNA synthetase was originally characterized as a tetramer based on dimethyl suberimidate chemical cross-linking experiments and analytical gel filtration chromatography[65] and has been cited in publications as being a tetramer[2,55,80−85] even after this conclusion was called into question in studies employing analytical ultracentrifugation and dynamic light scattering.[37,38] Given the importance of the oligomeric state of the protein in interpreting the affinity labeling experiments, in the analysis and interpretation of ligand binding, and in developing a model for the interaction of tRNA with the enzyme, we reexamined this issue using analytical gel filtration and analytical ultracentrifugation. Analysis of the purified wild-type enzyme (ARS875) on Superose 12 employing thyroglobulin, immunoglobulin G, human serum albumin, ovalbumin, and myoglobin as standards gave an apparent molecular weight of 245 000 (see Supporting Information Figure S1) which is in accord with values estimated by Sephadex G200 gel filtration.[86] This value is significantly lower than 384 000, the value expected for a tetramer formed from subunits of 95 898. The difference between this result and that reported[65] earlier may reflect the choice of standards, the nature of the gel filtration medium, and the fact that the separation is more a reflection of the Stokes radius or the radius of gyration rather than molecular weight. As will be shown from sedimentation velocity experiments, alanyl-tRNA synthetase is asymmetric, an attribute that would be reflected in the elution volume on gel filtration media. Analysis by sedimentation velocity in the analytical ultracentrifuge gave a value of ~7.2 S for $S_{20,w}$ extrapolated to zero concentration and values for molecular weight ranging from 160 000 to 180 000 based on the results

shown in the Supporting Information, Figures S2−S5. The dependence of *s* values on protein concentration is indicative of nonideal behavior, such as molecular asymmetry; similar concentration-dependent behavior was noted in the earlier studies.[38] Molecular weight estimated from the sedimentation velocity experiments shows concentration dependence consistent with a self-associating system. Sedimentation equilibrium studies at three protein concentrations and three speeds (shown in Supporting Information Figure S6) gave values for molecular weight ranging from 143 000 to 195 000, showing significant nonideal behavior. Data from the sedimentation equilibrium experiments from the lowest protein concentration where the nonideal behavior affects the results the least, shown in Figure 1, gave a molecular weight of 178 000−189 000,

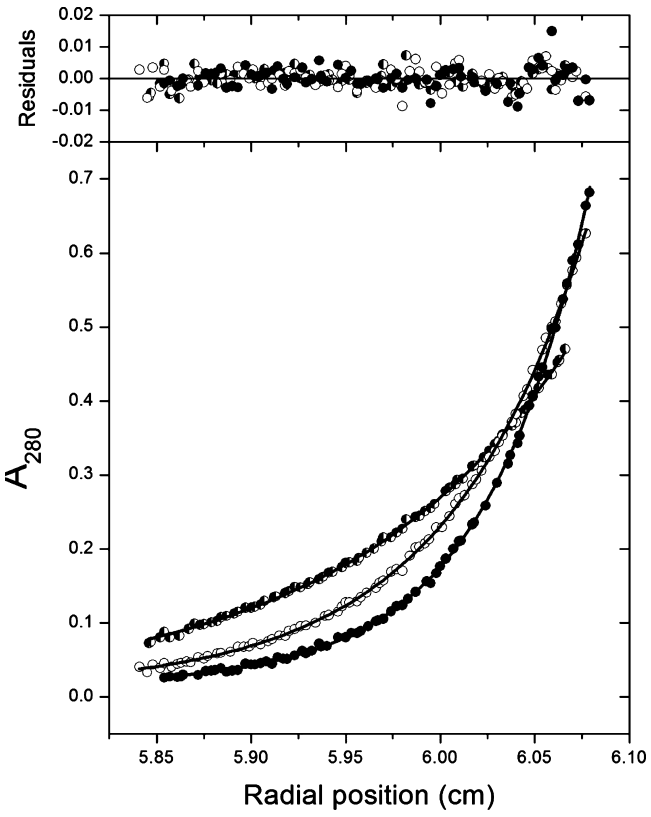

Figure 1. Sedimentation equilibrium. Data for a single loading concentration of $A_{280} \sim 0.2$ at three different rotor speeds of 8000 rpm (half-filled symbols), 10 000 rpm (open symbols), and 12 000 rpm (closed symbols) are shown. The curves represent fits to a single species model.

consistent with a predominant single dimeric species. The sedimentation experiments are described in detail in the Supporting Information and support the conclusion that alanyl-tRNA synthetase is predominantly a dimer in solution, in accord with the conclusions drawn from the earlier analytical ultracentrifugation and dynamic light scattering results.[37,38] There was no evidence of significant concentration of trimer or tetramer in the experiments described in the present work though in the earlier study there was evidence of self-association in a dimer−dodecamer equilibrium with the association to dodecamer being more pronounced at 10 °C.[38] Analysis of active, truncated forms of alanyl-tRNA synthetase containing the N-terminal 461 residues (ARS461) or the N-terminal 699 residues (ARS699) by analytical gel filtration on Superose 12 (shown in Supporting Information Figure S1) gave values of 62 000 and 73 000, respectively, consistent with their monomeric subunit molecular weights of 52 245 and 77 628 predicted from the amino acid sequence, assuming the N-terminal methionine is removed.

Binding of ATP, 5′-*O*-[*N*-(L-Glycinyl)sulfamoyl]-adenosine (GSAd), and 5′-*O*-[*N*-(L-alanyl)sulfamoyl]-adenosine (ASAd) to Alanyl-tRNA Synthetase. The binding of ATP and two adenylate analogues, GSAd and ASAd, were examined using isothermal titration calorimetry and enzyme assays. Figure 2 shows the results of titration calorimetry with ATP titrated into solutions of full length alanyl-tRNA synthetase (ARS875, panel A) and a deletion construct that is active in adenylate synthesis and aminoacylation of $tRNA^{ala}$ (ARS461, panel B). With both of these forms of alanyl-tRNA synthetase the binding was endothermic and was best fit with a single site binding model. Thermodynamic parameters for ATP derived from these experiments in Figure 2 are summarized in Table 1. The values of ΔH and ΔS were similar for the two proteins, and both gave stoichiometries close to 1.0 per subunit. There was no indication of cooperativity in the binding of ATP. For comparison, the value for ΔG for ATP (Table 1) was calculated from the K_m for ATP (95 μM) reported from a number of laboratories (range 80−140 μM with a mean of 94 ± 29),[62,87−89] assuming the value of K_m reflects the binding constant. The dissociation constants obtained from the ITC experiments shown in Figure 2a,b were 14.1 ± 0.5 μM for ARS875 and 23.9 ± 1.0 μM for ARS461; although these values are lower than the reported values of K_{ATP}, they lie in the same range as the Michaelis constants determined using an ATP-PP_i exchange assay.[62,87−89] The difference between the Michaelis constant for ATP ($K_{M,ATP}$) and the dissociation constant determined by calorimetry could result from $K_{M,ATP}$ being a complex kinetic parameter. If the system can be treated by the rapid equilibrium assumption, $K_{M,ATP}$ would approximate a dissociation constant for the binding of ATP to the enzyme−alanine complex and not to the unligated enzyme, as is the case for the dissociation constant determined from the ITC experiments. Binding of a noncognate aminoacyl-adenylate analogue, 5′-*O*-[*N*-(L-glycinyl)sulfamoyl]adenosine (GSAd), to full length alanyl-tRNA synthetase (Figure 2c) was strongly exothermic. The tight association of this compound puts in near the limit (6×10^{-9} M) for determination of a binding constant by ITC. The binding of cognate aminoacyl-adenylate analogue, (5′-*O*-[*N*-(L-alanyl)sulfamoyl]adenosine (ASAd), was also examined as shown in Figure 3A. As with GSAd and unlike ATP, binding of this nucleoside was strongly exothermic. The strong association of the alanyl-adenylate analogue (K_a significantly greater than 10^8 M^{-1}) precluded determination of its binding constants by ITC in the experiment shown in Figure 3A since there is essentially no free ligand during the course of titration until all the sites are occupied. The stoichiometries of ASAd and GSAd, 0.8 and 0.77, respectively, are consistent with the formation of 1:1 complexes of these nucleoside inhibitors with each subunit in the dimer. While the titration with ASAd cannot give an estimate of the binding constant, it does give an accurate estimate of the binding enthalpy. By examining the temperature dependence of ΔH, the heat capacity change (ΔC_p) upon binding of ASAd was determined as shown in Figure 3B; this value was large at −0.48 kcal mol^{-1} K^{-1}. When ASAd and GSAd were examined in enzymes assays, they were inhibitors at low concentrations as

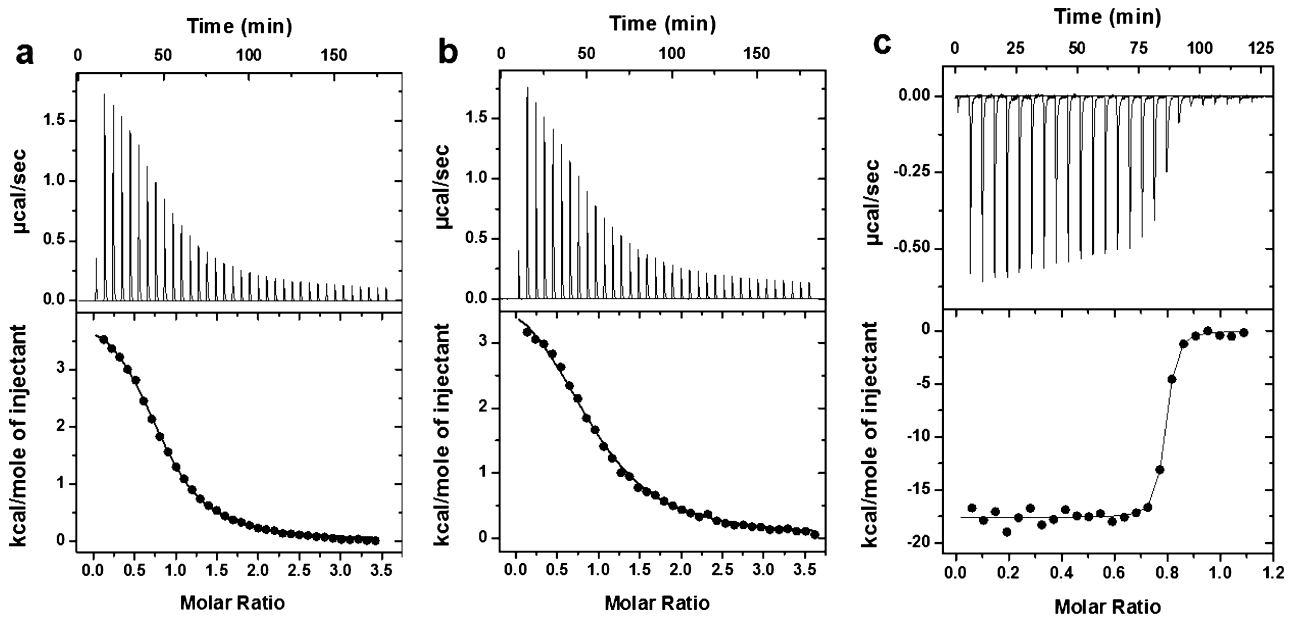

Figure 2. Isothermal titration calorimetry of ARS875 and ARS461 with Mg·ATP: (a) Mg·ATP (5 mM) was titrated into ARS875 (85 μM); (b) Mg·ATP (5 mM) was titrated into ARS461 (105 μM) at 25 °C as described in Experimental Procedures. The initial injection was 1 μL and subsequent injections were 3 μL in panels a and b. Titrations were performed at 25 °C. (c) GSAd (0.4 μM) was titrated into ARS875 (11.9 μM). The initial injection was 1 μL, and subsequent injections were 2 μL.

Table 1. Thermodynamic Parameters for Binding of Ligands to Alanyl-tRNA Synthetase

ligand	ΔG, kcal mol^{-1}	ΔH, kcal mol^{-1}	ΔS, cal deg^{-1} mol^{-1}	K_I, nM	stoich	T, K
ATP (ARS461)	−6.30 ± 0.03[a]	4.3 ± 0.12[a]	35.4[a]		0.94 ± 0.02	298
ATP (ARS875)	−6.61 ± 0.02[a]	4.18 ± 0.043[a]	36.2[a]		0.82 ± 0.02	298
ASAd	−14.0[b]	−18.8 ± 0.9[a]	−11.2[b]	0.2	0.8[a]	298
GSAd	−11.2 ± 0.2[a]	−17.6 ± 0.14[a]	−21.5[a]	4 ± 2	0.77[a]	298
ATP[c]	−5.6					303
alanine[c]	−4.8					303

[a]From ITC, present work. [b]Calculated from values for K_I from Figure 3 as described in the text. [c]Calculated from values for K_m of 95 μM for ATP and 340 μM for alanine.

shown in Figure 4 with ASAd being ~20 times more potent than GSAd, in keeping with the latter compound resembling the structure of noncognate glycyl-adenylate. Using the value for the binding constant for ATP determined by calorimetry, the concentration of ATP and alanine in the assay and assuming that these compounds bind as geometric inhibitors[90] that occupy both the ATP and alanine sites, values were calculated for the binding constants for these nucleosides (shown in Table 1). The inhibition constants calculated from the data in Figure 4 were 0.2 ± 0.1 and 4 ± 2 nM for ASAd and GSad, respectively. The K_I for ASAd may be lower since this value is less than the concentration of the enzyme in the assays, with the consequence that there is little free inhibitor. The value for the K_I for ASAd is an upper limit since the concentration of free inhibitor in the experiment is low due to its high affinity for the enzyme. In accord with the results of ITC, ASAd and GSAd are tight binding ligands with ASAd binding ~20-fold tighter than GSAd. We have assumed that these inhibitors bind in the adenylate forming site, though we have not ruled out binding in the editing site.

Modification of Alanyl-tRNA Synthetase with Periodate Oxidized tRNA^{ala}. We employed periodate oxidized tRNA^{ala} (otRNA^{ala}) as a probe to determine how other ligands affect the interaction of tRNA^{ala} with the enzyme and to identify residues in the enzyme that lie in proximity to the 3′-end of the bound tRNA^{ala}. As is shown later in this work, the dialdehyde of otRNA^{ala} reacts with lysyl residues of alanyl-tRNA synthetase to form a cyclic morpholine product that can be reduced to a stable adduct with $NaCNBH_3$.[91] The tRNA-modified forms of the protein have reduced mobility on SDS polyacrylamide gel electrophoresis. The results of such experiments are shown in Figure 5. Modification of the enzyme with otRNA^{ala} in the absence of other ligands (−ligand, panel A) gave at least five modified species, labeled a−e in Figure 5, when examined by SDS acrylamide gel electrophoresis. In the absence of other ligands, species e predominates. A faint species that is seen occasionally above species a is not labeled. The presence of alanine, AMP with alanine, or AMP alone had little discernible effect on the distribution of modified forms (Ala, AMP+ala, AMP in panel A) except that there is more unmodified protein when AMP is present. In modification reactions containing alanine and ATP (ATP+Ala in panel A), species b, c, and e predominate. Modification reactions with ATP present had predominantly species b and c. Modification of the enzyme with otRNA^{ala} was specific for this tRNA as two pools of fractions of *E. coli* tRNA purified by BD cellulose chromatography lacking acceptor activity for alanine, containing a mixture of noncognate tRNAs, gave little modification

dx.doi.org/10.1021/bi2012004 | *Biochemistry* 2011, 50, 9886−9900

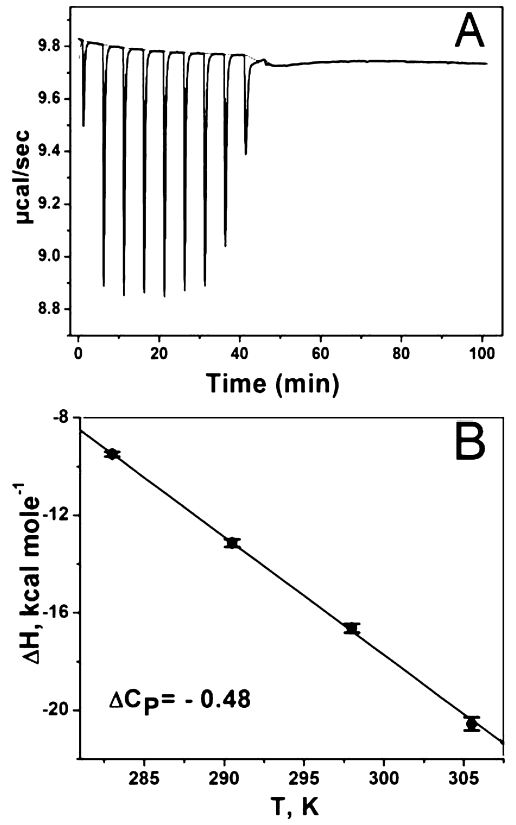

Figure 3. Isothermal titration calorimetry of ARS875 with ASAd: (A) ASAd (500 μM) was titrated into 10 μM ARS875 at 25 °C as described in the text; (B) heat capacity of ASAd binding. The enthalpy of ASAd binding to ARS875 was determined from injections of 500 μM ASAd into 10 μM ARS875 performed at the indicated temperatures. The initial injection was 1 μL, and subsequent injections were 2.5 μL.

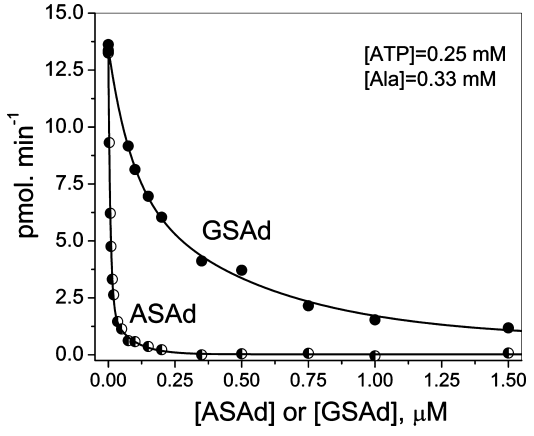

Figure 4. Inhibition of alanyl-tRNA synthetase by ASAd and GSAd. Assays were performed as described in Experimental Procedures.

(otRNA1 and otRNA2, Figure 5A). Periodate oxidation of the $tRNA^{ala}$ was required for modification and treating the modified enzyme with RNAase A returned the protein to its original electrophoretic mobility (data not shown). Two large species at approximately 160 000−180 000 molecular weight (labeled as X in Figure 5A) are consistently detected on SDS gel electrophoresis of the unmodified enzyme that was heated in the presence of mercaptoethanol. These components are not unrelated contaminants as they are made at elevated levels along with the 96 000 alanyl-tRNA synthetase polypeptide in cells harboring the expression vector employed for production of the protein. They also react with an antibody to alanyl-tRNA synthetase, and they exactly coelute with the enzyme activity and the 96 000 molecular weight polypeptide on various chromatographic media. Their mobility on SDS gel electrophoresis changes after incubation with $otRNA^{ala}$ (see top of the gel in Figure 5A) in a manner that parallels the modification of the 96 000 molecular weight polypeptide. We do not know the exact nature of these species but have detected them in every enzyme preparation; they appear to be aggregates of alanyl-tRNA synthetase that are not readily dissociated by moderate heat and SDS. These species are not seen in constructs ARS461 and ARS699 which lack the elements in the C-terminus that are involved in oligomerization. The $otRNA^{ala}$-modified alanyl-tRNA synthetase elutes from Superose 12 with a retention time corresponding to a molecular weight of 346 000 (Figure S1, Supporting Information), which is significantly larger than the values for singly (222 000) or doubly (247 000) modified enzyme predicted from amino acid sequence and the mass of the tRNA. This difference presumably reflects shape rather than a discrepancy in molecular weight. All of the modified species exactly coeluted in the chromatogram.

We examined the concentration dependence of ATP and AMP on modification of the enzyme by $otRNA^{ala}$ as shown in Figure 5B. The presence of ATP altered the distribution of modified species with a concentration dependence consistent with its dissociation constant (~0.02 mM). At high concentrations (5 mM and above), AMP elicits a similar effect. With both AMP and ATP there was a reduction in the component designated e, an increase in the species designated b and c, and an increase in the amount of unmodified enzyme. The alanyl-adenylate analogue, alanine sulfamoyl adenosine (ASAd in Figure 5B), gave a pattern in modification reactions similar to that observed at high ATP concentrations. Because ASAd binds essentially stoichiometrically to the enzyme under these conditions, it was not feasible to examine concentration dependence of this ligand in these experiments inasmuch as the enzyme is saturated with this ligand.

As shown in Figure 5C, the time course of appearance of the modified species was similar, with or without other ligands, indicating that one modified species is not likely a precursor to others. This experiment also illustrates the effect of the combination of ATP and alanine (ATP + alanine) that is not seen when these ligands are examined individually (ATP and alanine). Alanine alone had no discernible effect on the pattern of modification. Under the conditions employed for modification, the enzyme does form Ala-AMP.

To examine the extent to which C-terminal elements of alanyl-tRNA synthetase influences modification, we analyzed modification of a truncated form of the enzyme (ARS461) containing elements of the N-terminus, but lacking the C-terminal editing and oligomerization domains. This monomeric form of the enzyme has full activity in adenylate formation and aminoacylates $tRNA^{ala}$, though at a lower rate and with a higher dissociation constant for $tRNA^{ala}$.[39,40,42] An experiment examining the effect of ligands on modification of ARS461 by $otRNA^{ala}$ is shown in Figure 5D. Two modified species were detected in the absence of other ligands. To avoid confusion with the species identified in the full length enzyme, the species observed with ARS461 were designated α, β, and γ. In the absence of other ligands, primarily species α and γ are detected. In the presence of ATP, there is a reduction in the extent of

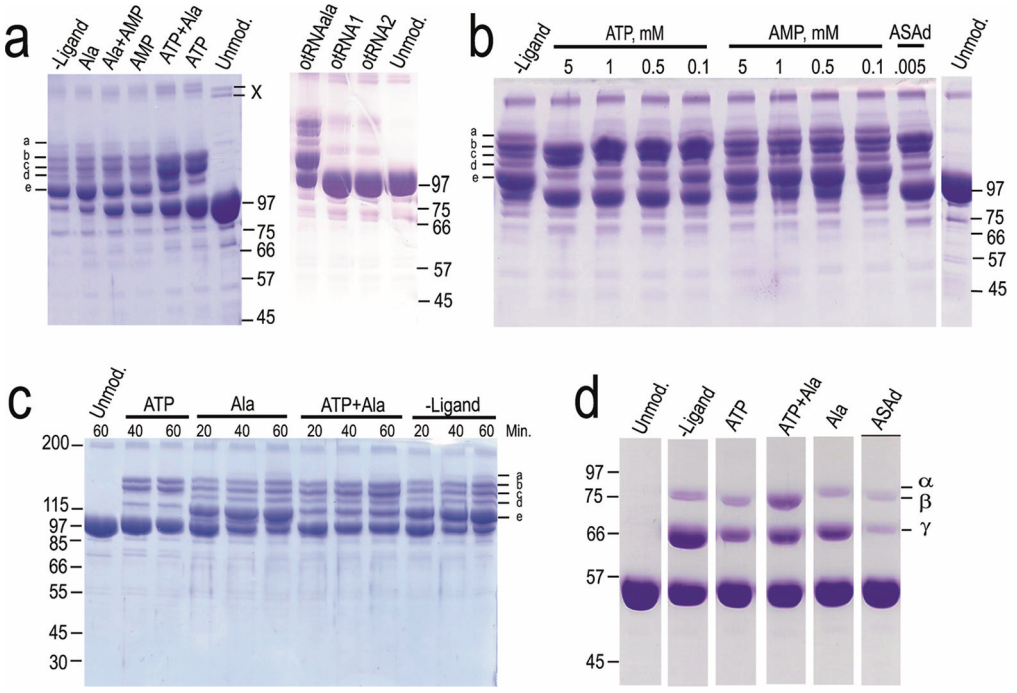

Figure 5. Effect of ligands on modification of *E. coli* alanyl-tRNA synthetase by otRNA^{ala}. Panel a (left): alanyl-tRNA synthetase (ARS875) was incubated with otRNA^{ala} and the indicated ligands for 1 h at 30 °C as described in Experimental Procedures. Mg·ATP (5 mM), AMP (5 mM), and alanine (2 mM) were added as indicated in the figure. Umod.: unmodified enzyme, incubated without otRNA^{ala}. Panel a (right): modification of alanyl-tRNA synthetase with noncognate tRNAs (otRNA1 and otRNA2); the first (otRNA^{ala}) and last (Unmod.) are positve and negative controls. Panel b: Effect of Mg·ATP, AMP, and GSAd on modification of alanyl-tRNA synthetase (ARS875) by otRNA^{ala}. Panel c: time course of modification of alanyl-tRNA synthetase (ARS875) in the presence of ATP, alanine, ATP + alanine, and without ligand (−ligand). Panel d: modification of alanyl-tRNA synthetase (ARS461) in the presence of ATP, ATP + alanine, alanine, and ASAd. Samples were incubated with otRNA^{ala} and the indicated ligands for 1 h at 30 °C as described in Experimental Procedures.

modification and a species with slightly faster mobility than α, designated β, is detected. In the presence of ATP and alanine, the concentration of β is increased. Alanine has little effect alone while ASAd greatly reduces the overall extent of modification and β is present rather than α. The otRNA^{ala}-modified ARS461 elutes from Superose 12 with a retention time corresponding to a molecular weight of 115 000 (see Figure S1, Supporting Information), significantly larger than the value expected for the singly modified protein (77 245). As with the full length protein, this difference presumably reflects shape rather than a discrepancy in molecular weight. The modified species (α, β, and γ) exactly coeluted in the chromatogram.

Identification of otRNA^{ala} Modification Sites in Alanyl-tRNA Synthetase. To identify the modification sites in alanyl-tRNA synthetase, enzyme was incubated with otRNA^{ala} with or without various ligands as described in Experimental Procedures. The modified enzyme was purified by gel filtration on Superose 12 to remove excess otRNA^{ala}. The purified, modified enzyme was digested with trypsin, and the tRNA^{ala}-peptides were purified by ion exchange chromatography on MonoQ. The tRNA^{ala}-peptides have slower migration than unmodified tRNA^{ala} in denaturing polyacrylamide gel electrophoresis (see Supporting Information Figure S7). After digestion with RNase A, the peptides were purified by C18 reversed-phase chromatography as shown in Figure 6; panel A shows the results of a control reaction employing a mixture of alanyl-tRNA synthetase and tRNA^{ala} that had not been periodate oxidized while panel B shows the results obtained with the otRNA^{ala}-modified enzyme. The HPLC chromatograms of the RNase A digested tRNA-peptides were compared to the chromatogram of the control reaction to identify components derived from the tRNA-peptides. The arrows with numbers in panel B of Figure 6 indicate the approximate elution position of modified peptides that were identified and sequenced by mass spectrometry. The peptide sequences are shown in Table 2; the number designations for the peptides correspond to the labels in Figure 6, panel B. Oxidation of otRNA^{ala} converts the 3′-ribose to a dialdehyde corresponding to **1** in Figure 7. Earlier studies[91] demonstrated that the reaction of sugars with vicinal diols oxidized to dialdehydes with primary amines generates a dihydromorpholine derivative (**2** in Figure 7) that can be reduced with sodium cyanoborohydride to form a stable morpholine (**3** in Figure 7). Reaction of the amine of lysyl residues on alanyl-tRNA synthetase with the dialdehyde on otRNA^{ala}, reduction with sodium cyanoborohydride, and digestion with RNAase A would be expected to give **4** in Figure 7. This modification of lysyl residues would render these sites resistant to trypsin. Six peptides from the C18 reversed-phase separation were detected with the masses expected for peptides derived from alanyl-tRNA synthetase with one missed tryptic cleavage at a lysyl-residue plus 233 mass units; the additional mass is that expected for the adenosine modification corresponding to **4** in Figure 7. The sequences derived from the mass spectrometric fragmentation analysis (shown in Supporting Information Figure S8, panels a–f) correspond to six potential tryptic peptides within the sequence of alanyl-tRNA synthetase. The properties and sequences of these peptides are summarized in Table 2, and their locations in the primary structure of the

dx.doi.org/10.1021/bi2012004 | *Biochemistry* 2011, 50, 9886–9900

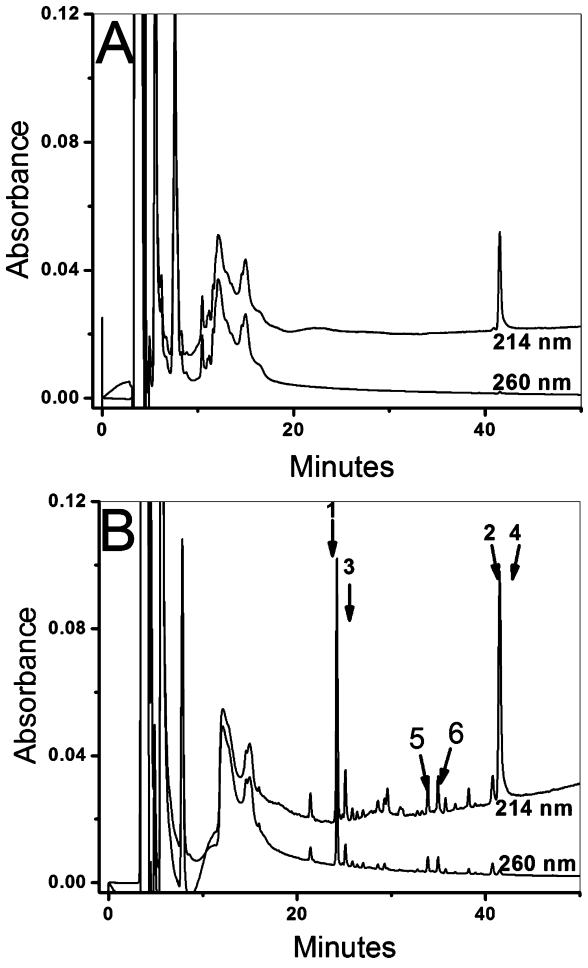

Figure 6. Reversed phase chromatography of $tRNA^{ala}$-peptides. Samples were prepared and subjected to chromatography on a C18 reversed phase column as described in the Experimental Procedures. Panel A: chromatography of digestion products from the control reaction. Panel B: chromatography of digestion products from the $tRNA^{ala}$-modified protein. Numbers above the arrows in panel B correspond to the number designations in Table 2.

protein are shown in Figure 8; the number designations correspond to the chromatogram in panel B of Figure 6. The mass of each of the modified peptides was 233 Da greater than their corresponding unmodified peptides. In the fragmentation of these modified peptides, there was an initial loss of 135 mass units corresponding to the labile base. This singly protonated, labile fragment can be seen in the tandem mass spectra as a peak at m/z 136 (labeled with an asterisk in the mass spectra shown Supporting Information Figure S8). After the initial base loss, fragment ions could be matched to tryptic peptides from the sequence of the alanyl-tRNA synthetase but were 98 mass units greater than the mass of the peptide containing the unmodified lysine. Previous work on the mass spectrometric fragmentation of nucleotides[92,93] demonstrated that the base is labile, and its loss gives **5** in Figure 7; the mass of the product after loss of the adenosine is 98, in keeping with the difference in mass between the fragmentation products seen in the mass spectra (shown in Figure S8 in Supporting Information). One of the peptides detected in these experiments lying near the N-terminus (modification at residue 74) was identified earlier.[62] The other five modification sites, which lie in the editing domain, were not identified previously. Modification at residue 74 likely corresponds to the major species (e in Figure 5) seen on SDS polyacrylamide gel electrophoresis of modification products obtained in the absence of other ligands. We also examined the modification products obtained with ARS461 using the same strategy that was employed for the full length protein. There are three major products whose relative abundance is altered by the presence of ligands. Five of the modification sites in ARS875 identified by mass spectrometry lie in structures not present in ARS461, suggesting that there must be at least one and possibly two sites in ARS461 in addition to lysine 74. Our sequence analysis identified lysine 74 as a modification site in peptides derived from otRNA-modified ARS461, but no other modified peptides were identified (data not shown).

DISCUSSION

E. coli alanyl-tRNA synthetase is a dimer of identical subunits, similar to other bacterial[94] and archeal alanyl-tRNA synthetases.[53] A dimer−dodecamer self-association[38] may account in part for the earlier report of it being a tetramer[65] since a self-associating system would elute as a single zone upon gel filtration chromatography; the effect of temperature reported in the earlier analytical ultracentrifugation analysis suggests that the dodecamer would be favored at lower temperatures. Asymmetry of the protein, as indicated by the sedimentation velocity experiments, may also have contributed to the earlier conclusion. Eukaryotic alanyl-tRNA synthetases[68,95−97] differ from their bacterial and archeal counterparts in that they are monomers. Gly to asp mutations at residues 675 and 678 (674 T**G**DI**G**L 679) result in monomeric, full length proteins[98] with reduced aminoacyl-tRNA synthetase activity. Adenylate formation was not affected, implying that oligomeric state influenced $tRNA^{ala}$ binding or transfer of alanine from alanyl-adenylate to $tRNA^{ala}$. These glycyl residues are conserved in structures of the *Archeoglobus fulgidus* (711 T**G**EI**G**M 716) and *Pyrococcus horikoshii* (725 T**G**LV**G**P 730) enzymes.

Table 2. Sequence of Modified Peptides from $otRNA^{ala}$-Modified *E. coli* Alanyl-tRNA Synthetase[a]

	m/z	charge	obsd MH^{+1}_{mono}	pred MH^{+1}_{mono}	sequence
1	645.70	+3	1935.10	1701.83	71 AGG**K**HNDLEN VGYTAR 86
2	891.03	+3	2671.09	2438.21	514 GANFSFAVED TQ**K**YGQAIGH IGK 536
3	681.75	+3	2043.25	1809.98	576 QVLGTHVSQ**K** GSLVNDK 592
4	1052.44	+2	2103.88	1870.99	623 NLPIETNIMD LEAA**K**AK 639
5	686.31	+2	1371.62	1138.59	638 A**K**GAM$_{ox}$ALFGE K 658
6	868.36	+2	1735.72	1502.69	640 GAM$_{ox}$ALFGE**K**Y DERVR 654

[a]Residue numbers are based on the predicted amino acid sequence which includes the N-terminal methionine; the N-terminal methionine is absent in the mature protein. Modified lysyl residues detected by mass spectrometry are indicated in bold and underlined. Predicted mass is based on the monisotopic mass. M_{ox} indicates oxidized methionine.

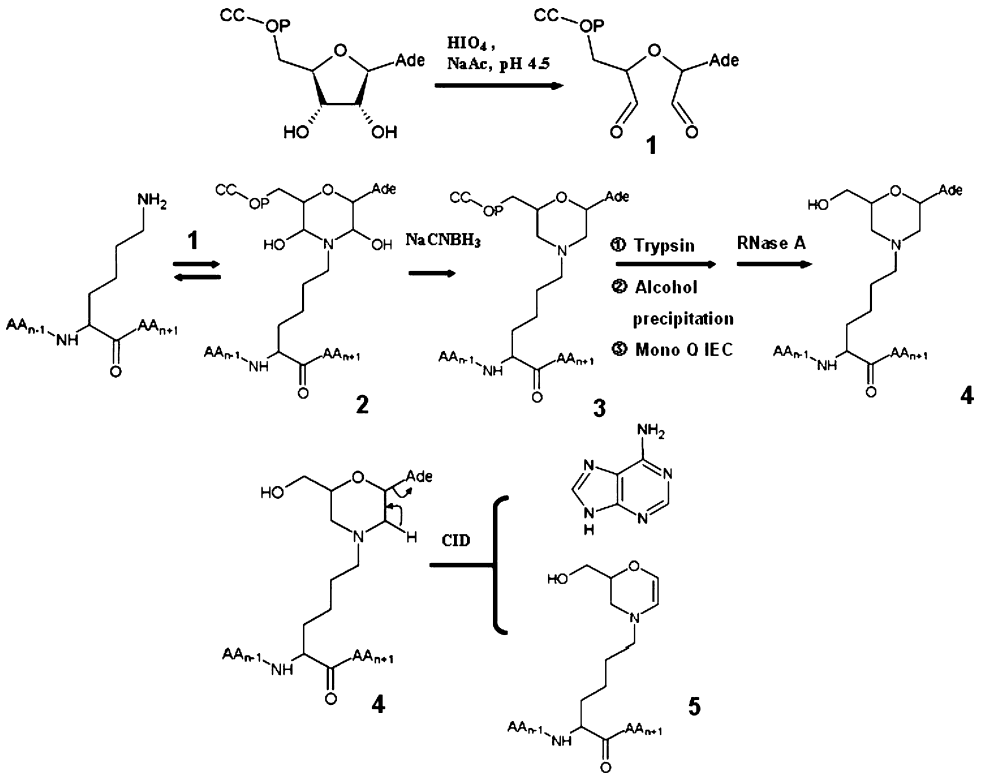

Figure 7. Scheme for modification of alanyl-tRNA synthetase with otRNA, peptide isolation, and analysis by mass spectrometry. See the text for details. IEC is ion exchange chromatography; CID is collision induced dissociation.

```
1    MSKSTAEIRQ AFLDFFHSKG HQVVASSSLV PHNDPTLLFT NAGMNQFKDV FLGLDKRNYS 60
61   RATTSQRCVR AGGKHNDLEN VGYTARHHTF FEMLGNFSFG DYFKHDAIQF AWELLTSEKW 120
121  FALPKERLWV TVYESDDEAY EIWEKEVGIP RERIIRIGDN KGAPYASDNF WQMGDTGPCG 180
181  PCTEIFYDHG DHIWGGPPGS PEEDGDRYIE IWNIVFMQFN RQADGTMEPL PKPSVDTGMG 240
241  LERIAAVLQH VNSNYDIDLF RTLIQAVAKV TGATDLSNKS LRVIADHIRS CAFLIADGVM 300
301  PSNENRGYVL RRIIRRAVRH GNMLGAKETF FYKLVGPLID VMGSAGEDLK RQQAQVEQVL 360
361  KTEEEQFART LERGLALLDE ELAKLSGDTL DGETAFRLYD TYGFPVDLTA DVCRERNIKV 420
421  DEAGFEAAME EQRRRAREAS GFGADYNAMI RVDSASEFKG YDHLELNGKV TALFVDGKAV 480
481  DAINAGQEAV VVLDQTPFYA ESGGQVGDKG ELKGANFSFA VEDTQKYGQA IGHIGKLAAG 540
541  SLKVGDAVQA DVDEARRARI RLNHSATHLM HAALRQVLGT HVSQKGSLVN DKVLRFDFSH 600
601  NEAMKPEEIR AVEDLVNTQI RRNLPIETNI MDLEAAKAKG AMALFGEKYD ERVRVLSMGD 660
661  FSTELCGGTH ASRTGDIGLF RIISESGTAA GVRRIEAVTG EGAIATVHAD SDRLSEVAHL 720
721  LKGDSNNLAD KVRSVLERTR QLEKELQQLK EQAAAQESAN LSSKAIDVNG VKLLVSKLSG 780
781  VEPKMLRTMV DDLKNQLGST IIVLATVVEG KVSLIAGVSK DVTDRVKAGE LIGMVAQQVG 840
841  GKGGGRPDMA QAGGTDAAAL PAALASVKGW VSAKLQ
```

Figure 8. Location of peptides identified by mass spectrometry in the sequence of alanyl-tRNA synthetase. Peptides identified by mass spectrometry are indicated by horizontal bars under the sequence. The modified lysyl residues in the peptides are underlined. The deduced amino acid sequence of alanyl-tRNA synthetase comes from GenBank accession number NC012967.

ATP binding is endothermic with no indication of cooperativity in the absence of tRNA and amino acid; thermodynamic parameters were virtually identical with the full-length enzyme (ARS875) and with a construct consisting of the amino-terminal elements (ARS461) required for adenylate synthesis and aminoacylation. The binding of the adenylate analogues ASAd and GSAd is energetically distinct from ATP, inasmuch as binding is decidedly exothermic. The tight binding of the noncognate GSAd adenylate analogue underscores the necessity for an editing activity in maintaining the fidelity of aminoacylation. The large heat capacity change (ΔC_p = 0.48 kcal mol^{-1} K^{-1}) associated with ASAd binding suggests that a conformational change is associated with binding of this ligand and likely with formation of the alanyl-adenylate intermediate.

dx.doi.org/10.1021/bi2012004 | *Biochemistry* 2011, 50, 9886–9900

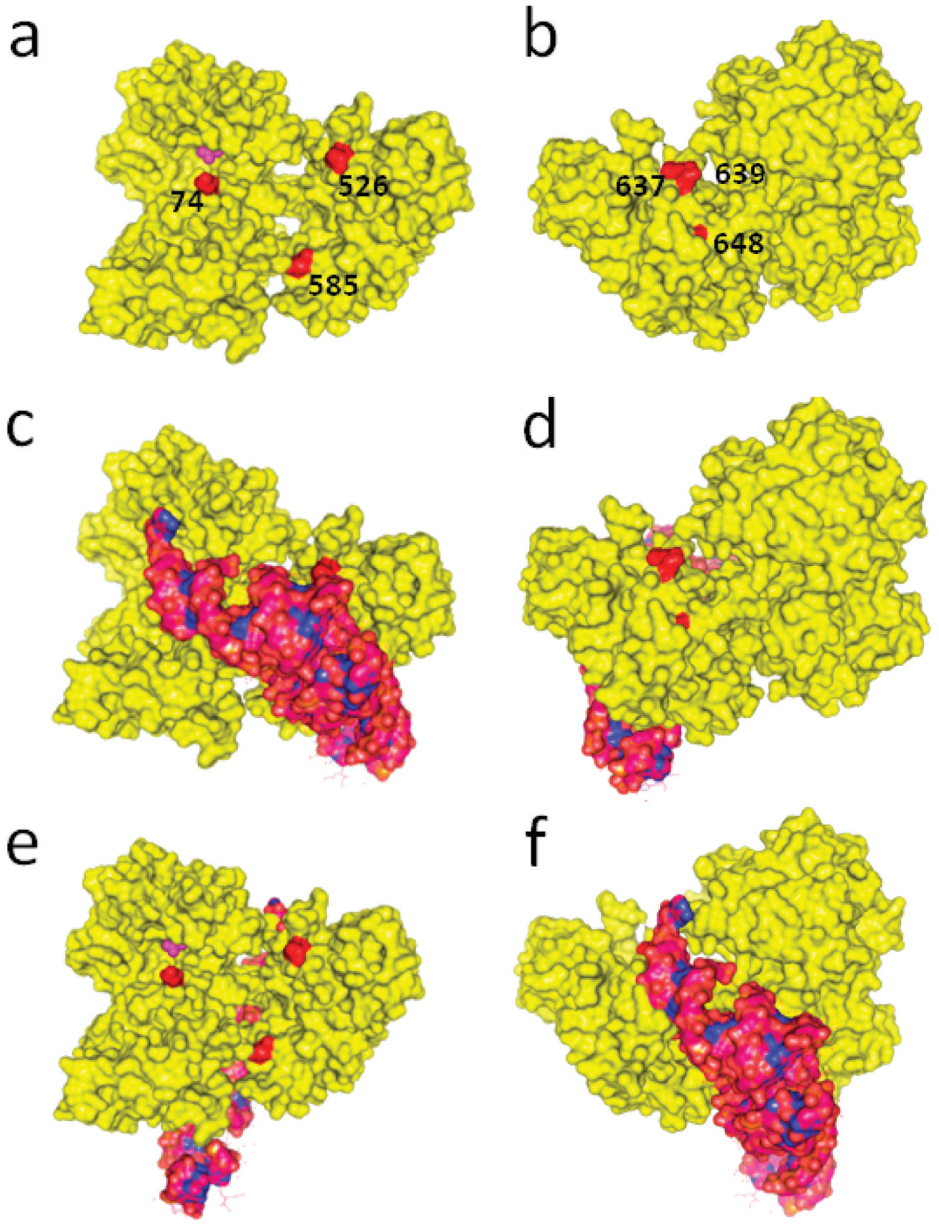

Figure 9. Alanyl-tRNA synthetase structure. Surface renderings of alanyl-tRNA synthetase are based on the structure of the N-terminal aminoacylation domain and the primary structure of *E. coli* alanyl-tRNA synthetase editing domain superimposed on the known structure of the enzyme from *A. fulgidus*. Lysines 74, 526, 585, 637, 639, and 648 are indicated in red. Panels c–f are the structures with tRNA docked on the enzyme in two different orientations as described in the text. The structures shown in the panels on the right side of the figure are rotated 180° with respect to those shown on the left side. Alanine bound at the active site in panels a and e is shown is shown colored cyan.

Large heat capacity changes have been correlated empirically with a change in solvent accessible surface area by comparing structures of ligand–protein complexes with the structures of the unligated forms.[99] Large heat capacity changes are thought to reflect the burial of hydrophobic residues in the complex.

Alanyl-tRNA synthetase can be modified specifically with otRNA^{ala} at multiple sites. We exploited this property to determine how the 3′-acceptor end of tRNA^{ala} is oriented on the enzyme surface. The location of the six sites identified in the present study are shown in red in Figure 9. One site (lys 74) lies on a beta turn at the opening to the adenylate forming site in the aminoacylation domain and two sites (lys 526 and lys 585) lie in the editing domain as shown in red in Figure 9a (left panel). Three modification sites (lys 637, 639 and lys 648) lie clustered on the backside of the editing domain as shown in Figure 9b (right panel). The modification experiments suggest that occupation of the ATP and alanine binding sites influence how the tRNA is oriented on the enzyme surface presumably through conformational transitions linked to ligand binding. The modification site (lys 74) identified and sequenced by mass spectrometry in the present study corresponds to that identified in earlier work.[62] The 3′-end of tRNA^{ala} interacting with residues in the aminoacylation domain, as reflected by modification of lysine 74, is eminently sensible since the tRNA would be oriented to react with the adenylate in the active site as shown in Figure 9c. However, there is also modification at sites near the opening to the editing domain (lys 526 and lys 585) which would require that the tRNA be rotated ~90°. The corresponding residues in the archeal enzymes (E564 and A636 in *A. fulgidus* and K577 and A636 in *P. horikoshii*) lie on beta

dx.doi.org/10.1021/bi2012004 | *Biochemistry* 2011, 50, 9886–9900

stands on two sides of the opening to the editing site. One might expect the editing site to be occupied by the 3′-end of the misacylated $tRNA^{ala}$ with the unacylated $tRNA^{ala}$ residing in the aminoacylation domain. However, the result is consistent with a model proposed by Francklyn[63] which has the enzyme assuming four states: state 1 is apoenzyme lacking ligands; state 2 is a resting state with the enzyme complexed with tRNA with its CCA terminus in the editing site; state 3 is a synthetic mode in which tRNA translocates from the editing site to react with adenylate in the active site; and state 4 is an editing mode in which aminoacyl-tRNA translocates to the editing site for inspection, in the case of the cognate aminoacyl-tRNA, or hydrolysis in the case of the misacylated tRNA. The absence or presence of ligands appears to alter the relative distribution of conformers with the CCA terminus in one site or the other. On the basis of crystal structures of the tRNA−enzyme complex, threonyl-tRNA synthetase has been proposed as a model for class 2 enzymes that have an editing domain. In the absence of other ligands, the CCA terminus of $tRNA^{thr}$ resides in the catalytic pocket of the aminoacylation domain.[100] Analysis of the structures of enzyme−ligand complexes of *Staphylococcus aureus* threonyl-tRNA synthetase indicate that threonine and ATP must be bound before productive binding of $tRNA^{thr}$.[28] Dock-Bregeon et al. proposed that the CCA terminus of the misacylated $tRNA^{thr}$ (e.g., Ser-$tRNA^{thr}$) undergoes a conformational transition from a helical conformation to a hairpin structure as it translocates 39 Å to the editing site.[64] The present studies on alanyl-tRNA synthetase are consistent with the CCA terminus residing primarily in the aminoacylation site in the absence of other ligands; the distribution changes in the presence of ATP or an adenylate analogue. The editing domain of alanyl-tRNA-synthetase lies C-terminal with respect to the aminoacylation domain,[53] while the editing domain in threonyl tRNA-synthetase lies on the opposite side, N-terminal with respect to the aminoacylation domain. It is difficult to reconcile tRNA and aminoacyl-tRNA binding to these two structures in similar orientations.

Three modification sites (lys 637, lys 639, and lys 648) lie on the back side of the editing domain as shown in Figure 9b,d. Interaction of the 3′-end of the tRNA with these sites appears to require association of $tRNA^{ala}$ with the enzyme in a different mode from that shown in Figure 9c. Two of the modification sites, K637 and K639, lie on what corresponds to an exposed α helix (residues E673 and K675) in the *A. fulgidus* protein. One concern is that these modification sites might reflect nonspecific interaction. However, these sites lie in close proximity, a result that is not consistent with nonspecific modification. In addition, significant modification of alanyl-tRNA synthetase was not seen with noncognate tRNA. Although one could propose that $tRNA^{ala}$ associates in any number of orientations that place the 3′-terminus in proximity to these sites, one potential orientation is displayed in Figure 9f. The ultimate question is what role does this interaction play in the function of the enzyme. The role of this site may be regulatory rather than catalytic inasmuch as the 3′-end of the tRNA does not lie near the editing or the aminoacylation site. In this vein, while the exact function of the C-terminal globular domain of alanyl-tRNA synthetase is poorly defined, it is functionally important as its removal reduces the activity of the *A. fulgidus* and *E. coli* enzymes and reduces the editing efficiency of the *E. coli* enzyme. Defining the mode of interaction of $tRNA^{ala}$ with alanyl-tRNA synthetase will require acquiring structures of a $tRNA^{ala}$-alanyl-tRNA synthetase complex; this may be challenging if, as our data indicates, the tRNA−enzyme complex is dynamic. An added complexity that we have not addressed is the likely flexible nature of the connection between the adenylate forming domain and the editing domain. It is possible that the domains move significantly, a feature that would not be reflected in the crystal structure. Additionally, because the subunits in the dimer are linked through a C-terminal a coiled-coil structure, there might be interaction between the two adenylate-editing structures of the dimer.

■ ASSOCIATED CONTENT

Ⓢ Supporting Information

Analytical gel filtration; sedimentation velocity and sedimentation equilibrium analytical ultracentrifugation; purification of $tRNA^{ala}$-peptides; peptide mass spectra. This material is available free of charge via the Internet at http://pubs.acs.org.

Accession Codes

Alanyl-tRNA synthetase protein sequences were from GenBank NC012967. The structures of alanyl-tRNA synthetase from *A. fulgidus* was from PDB 2ZTG. The structure of the *E. coli* alanyl-tRNA synthetase adenylate synthesis domain was from PDB 3HXU.

■ AUTHOR INFORMATION

Corresponding Author

*Phone: 419-383-4136. Fax: 419-383-6228. E-mail: david.dignam@utoledo.edu.

■ ACKNOWLEDGMENTS

We are grateful to Max O. Funk for the use of his VP-ITC calorimeter.

■ ABBREVIATIONS

ASAd, (5′-*O*-[*N*-(L-alanyl)sulfamoyl]adenosine; ACN, acetonitrile; GSAd, 5′-*O*-[*N*-(L-glycinyl)sulfamoyl]adenosine; ARS875, alanyl-tRNA synthetase residues 1−875; ARS461, alanyl-tRNA synthetase residues 1−461; BD cellulose, benzyolated diethylaminoethyl cellulose; DTT, dithiothreitol; EDTA, ethylenediaminotetraacetate; MOPS, 3-(*N*-morpholino)-propanesulfonic acid; $otRNA^{ala}$, $tRNA^{ala}$ with the 3′-ribose oxidized with sodium periodate to a dialdehyde; PMSF, phenylmethylsulfonyl fluoride; SDS, sodium dodecyl sulfate; SE, sedimentation equilibrium; SV, sedimentation velocity; TFA, trifluoroacetic acid; TFA, trifluoroacetic acid.

■ REFERENCES

(1) Ling, J., Roy, H., and Ibba, M. (2007) Mechanism of tRNA-dependent editing in translational quality control. *Proc. Natl. Acad. Sci. U. S. A. 104*, 72−77.

(2) Ibba, M., and Söll, D. (2000) Aminoacyl-tRNA synthesis. *Annu. Rev. Biochem. 69*, 617−650.

(3) Ibba, M., and Söll, D. (2001) The renaissance of aminoacyl-tRNA synthesis. *EMBO Rep. 2*, 382−387.

(4) Ataide, S. F., and Ibba, M. (2006) Small molecules: big players in the evolution of protein synthesis. *ACS Chem. Biol. 1*, 285−297.

(5) Ibba, M., and Söll, D. (2004) Aminoacyl-tRNAs: setting the limits of the genetic code. *Genes Dev. 18*, 731−738.

(6) Schimmel, P. (1990) Alanine transfer RNA synthetase: structure-function relationships and molecular recognition of transfer RNA. *Adv. Enzymol. Relat. Areas Mol. Biol. 63*, 233−270.

(7) Hoagland, M. B., Stephenson, M. L., Scott, J. F., Hecht, L. I., and Zamecnik, P. C. (1958) A soluble ribonucleic acid intermediate in protein synthesis. *J. Biol. Chem. 231*, 241−257.

(8) Zamecnik, P. C., Keller, E. B., Littlefield, J. W., Hoagland, M. B., and Loftfield, R. B. (1956) Mechanism of incorporation of labeled amino acids into protein. *J. Cell. Physiol. Suppl. 47*, 81−101.
(9) Hoagland, M. B., Keller, E. B., and Zamecnik, P. C. (1956) Enzymatic carboxyl activation of amino acids. *J. Biol. Chem. 218*, 345−358.
(10) Koshland, D. E., Nemethy, G., and Filmer, D. (1966) Comparison of experimental binding data and theoretical models in proteins containing subunits. *Biochemistry 5*, 365−385.
(11) Zhou, M., Azzi, A., Xia, X., Wang, E. D., and Lin, S. X. (2006) Crystallization and preliminary X-ray diffraction analysis of E. coli arginyl-tRNA synthetase in complex form with a tRNA(Arg). *Amino Acids 32*, 479−482.
(12) Guigou, L., and Mirande, M. (2005) Determinants in tRNA for activation of arginyl-tRNA synthetase: evidence that tRNA flexibility is required for the induced-fit mechanism. *Biochemistry 44*, 16540−16548.
(13) Shimada, A., Nureki, O., Goto, M., Takahashi, S., and Yokoyama, S. (2001) Structural and mutational studies of the recognition of the arginine tRNA-specific major identity element, A20, by arginyl-tRNA synthetase. *Proc. Natl. Acad. Sci. U. S. A. 98*, 13537−13542.
(14) Delagoutte, B., Moras, D., and Cavarelli, J. (2000) tRNA aminoacylation by arginyl-tRNA synthetase: induced conformations during substrates binding. *EMBO J. 19*, 5599−5610.
(15) Simader, H., Hothorn, M., Kohler, C., Basquin, J., Simos, G., and Suck, D. (2006) Structural basis of yeast aminoacyl-tRNA synthetase complex formation revealed by crystal structures of two binary sub-complexes. *Nucleic Acids Res. 34*, 3968−3979.
(16) Sekine, S., Shichiri, M., Bernier, S., Chenevert, R., Lapointe, J., and Yokoyama, S. (2006) Structural bases of transfer RNA-dependent amino acid recognition and activation by glutamyl-tRNA synthetase. *Structure 14*, 1791−1799.
(17) Freist, W., Gauss, D. H., Söll, D., and Lapointe, J. (1997) Glutamyl-tRNA sythetase. *Biol. Chem. 378*, 1313−1329.
(18) Sekine, S., Nureki, O., Dubois, D. Y., Bernier, S., Chenevert, R., Lapointe, J., Vassylyev, D. G., and Yokoyama, S. (2003) ATP binding by glutamyl-tRNA synthetase is switched to the productive mode by tRNA binding. *EMBO J. 22*, 676−688.
(19) Uter, N. T., and Perona, J. J. (2006) Active-site assembly in glutaminyl-tRNA synthetase by tRNA-mediated induced fit. *Biochemistry 45*, 6858−6865.
(20) Uter, N. T., Gruic-Sovulj, I., and Perona, J. J. (2005) Amino acid-dependent transfer RNA affinity in a class I aminoacyl-tRNA synthetase. *J. Biol. Chem. 280*, 23966−23977.
(21) Uter, N. T., and Perona, J. J. (2004) Long-range intramolecular signaling in a tRNA synthetase complex revealed by pre-steady-state kinetics. *Proc. Natl. Acad. Sci. U. S. A. 101*, 14396−14401.
(22) Roy, S. (2004) Fluorescence quenching methods to study protein-nucleic acid interactions. *Methods Enzymol. 379*, 175−187.
(23) Sherlin, L. D., and Perona, J. J. (2003) tRNA-dependent active site assembly in a class I aminoacyl-tRNA synthetase. *Structure 11*, 591−603.
(24) Cusack, S., Yaremchuk, A., and Tukalo, M. (1996) The crystal structure of the ternary complex of T.thermophilus seryl-tRNA synthetase with tRNA(Ser) and a seryl-adenylate analogue reveals a conformational switch in the active site. *EMBO J. 15*, 2834−2842.
(25) Gruic-Sovulj, I., Landeka, I., Soll, D., and Weygand-Durasevic, I. (2002) tRNA-dependent amino acid discrimination by yeast seryl-tRNA synthetase. *Eur. J. Biochem. 269*, 5271−5279.
(26) Gruic-Sovulj, I., Ludemann, H. C., Hillenkamp, F., Kucan, I., and Peter-Katalinic, J. (1997) Detection of noncovalent tRNA.aminoacyl-tRNA synthetase complexes by matrix-assisted laser desorption/ionization mass spectrometry. *J. Biol. Chem. 272*, 32084−32091.
(27) Minajigi, A., and Francklyn, C. S. (2010) Amionacyl tranfer rate dictates choice of editing pathway in threonyl-tRNA synthetase. *J. Biol. Chem. 285*, 23810−23817.
(28) Torres-Larios, A., Sankaranarayanan, R., Rees, B., Dock-Bregeon, A. C., and Moras, D. (2003) Conformational movements and cooperativity upon amino acid, ATP and tRNA binding in threonyl-tRNA synthetase. *J. Mol. Biol. 331*, 201−211.
(29) Freist, W., and Gauss, D. H. (1995) Threonyl-tRNA synthetase. *Biol. Chem. Hoppe Seyler 376*, 213−224.
(30) Briand, C., Poterszman, A., Eiler, S., Webster, G., Thierry, J., and Moras, D. (2000) An intermediate step in the recognition of tRNA(Asp) by aspartyl-tRNA synthetase. *J. Mol. Biol. 299*, 1051−1060.
(31) Moulinier, L., Eiler, S., Eriani, G., Gangloff, J., Thierry, J. C., Gabriel, K., McClain, W. H., and Moras, D. (2001) The structure of an AspRS-tRNA(Asp) complex reveals a tRNA-dependent control mechanism. *EMBO J. 20*, 5290−5301.
(32) Sauter, C., Lorber, B., Cavarelli, J., Moras, D., and Giege, R. (2000) The free yeast aspartyl-tRNA synthetase differs from the tRNA(Asp)-complexed enzyme by structural changes in the catalytic site, hinge region, and anticodon-binding domain. *J. Mol. Biol. 299*, 1313−1324.
(33) Rees, B., Webster, G., Delarue, M., Boeglin, M., and Moras, D. (2000) Aspartyl tRNA-synthetase from Escherichia coli: flexibility and adaptability to the substrates. *J. Mol. Biol. 299*, 1157−1164.
(34) Yaremchuk, A., Tukalo, M., Grotli, M., and Cusack, S. (2001) A succession of substrate induced conformational changes ensures the amino acid specificity of Thermus thermophilus prolyl-tRNA synthetase: comparison with histidyl-tRNA synthetase. *J. Mol. Biol. 309*, 989−1002.
(35) Cusack, S. (1997) Aminoacyl-tRNA synthetases. *Curr. Opin. Struct. Biol. 7*, 881−889.
(36) Eriani, G., Delarue, M., Poch, O., Gangloff, J., and Moras, D. (1990) Partition of tRNA synthetases into two classes based on mutually exclusive sets of sequence motifs. *Nature 347*, 203−206.
(37) Sood, S. M., Hill, K. A., and Slattery, C. W. (1997) Stability of Escherichia coli alanyl-tRNA synthetase quaternary structure under increased pressure. *Arch. Biochem. Biophys. 346*, 322−323.
(38) Sood, S. M., Slattery, C. W., Filley, S. J., Wu, M. X., and Hill, K. A. (1996) Further characterization of Escherichia coli alanyl-tRNA synthetase. *Arch. Biochem. Biophys. 328*, 295−301.
(39) Jasin, M., Regan, L., and Schimmel, P. (1983) Modular arrangement of functional domains along the sequence of an aminoacyl tRNA synthetase. *Nature 306*, 441−447.
(40) Jasin, M., Regan, L., and Schimmel, P. (1984) Dispensable pieces of an aminoacyl tRNA synthetase which activate the catalytic site. *Cell 36*, 1089−1095.
(41) Putney, S. D., Royal, N. J., Neuman de Vegvar, H., Herlihy, W. C., Biemann, K., and Schimmel, P. (1981) Primary structure of a large aminoacyl-tRNA synthetase. *Science 213*, 1497−1501.
(42) Regan, L., Bowie, J., and Schimmel, P. (1987) Polypeptide sequences essential for RNA recognition by an enzyme. *Science 235*, 1651−1653.
(43) Beebe, K., Mock, M., Merriman, E., and Schimmel, P. (2008) Distinct domains of tRNA synthetase recognize the same base pair. *Nature 451*, 90−93.
(44) Tsui, W. C., and Fersht, A. R. (1981) Probing the principles of amino acid selection using the alanyl-tRNA synthetase from Escherichia coli. *Nucleic Acids Res. 9*, 4627−4637.
(45) Baldwin, A. N., and Berg, P. (1966) Transfer ribonucleic acid-induced hydrolysis of valyladenylate bound to isoleucyl ribonucleic acid synthetase. *J. Biol. Chem. 241*, 839−845.
(46) Beuning, P. J., and Musier-Forsyth, K. (2000) Hydrolytic editing by a class II aminoacyl-tRNA synthetase. *Proc. Natl. Acad. Sci. U. S. A. 97*, 8916−8920.
(47) Farrow, M. A., Nordin, B. E., and Schimmel, P. (1999) Nucleotide determinants for tRNA-dependent amino acid discrimination by a class I tRNA synthetase. *Biochemistry 38*, 16898−16903.
(48) Hale, S. P., Auld, D. S., Schmidt, E., and Schimmel, P. (1997) Discrete determinants in transfer RNA for editing and aminoacylation. *Science 276*, 1250−1252.
(49) Schmidt, E., and Schimmel, P. (1994) Mutational isolation of a sieve for editing in a transfer RNA synthetase. *Science 264*, 265−267.

(50) Hati, S., Ziervogel, B., Sternjohn, J., Wong, F. C., Nagan, M. C., Rosen, A. E., Siliciano, P. G., Chihade, J. W., and Musier-Forsyth, K. (2006) Pre-transfer editing by class II prolyl-tRNA synthetase: role of aminoacylation active site in "selective release" of noncognate amino acids. *J. Biol. Chem. 281*, 27862−27872.

(51) Betha, A. K., Williams, A. M., and Martinis, S. A. (2007) Isolated CP1 domain of Escherichia coli leucyl-tRNA synthetase is dependent on flanking hinge motifs for amino acid editing activity. *Biochemistry 46*, 6258−6267.

(52) Dulic, M., Cvetesic, N., Perona, J. J., and Gruic-Sovulj, I. (2010) Partitioning of tRNA-dependent editing between pre- and post-transfer pathways in class I aminoacyl-tRNA synthetases. *J. Biol. Chem. 285*, 23799−23809.

(53) Naganuma, M., Sekine, S.-i., Fukunaga, R., and Yokoyama, S. (2009) Unique protein architecture of alanyl-tRNA synthetase for aminoacylation, editing, and dimerization. *Proc. Natl. Acad. Sci. U. S. A. 106*, 8489−8494.

(54) Guo, M., Chong, Y. E., Beebe, K., Shapiro, R., Yang, X.-L., and Schimmel, P. (2009) The C-Ala domain brings together editing and aminoacylation functions on one tRNA. *Science 325*, 744−747.

(55) Sokabe, M., Ose, T., Nakamura, T. A., Tokunaga, K., Nureki, O., Yao, M., and Tanaka, I. (2009) The structure of alanyl-tRNA synthetase with editing domain. *Proc. Natl. Acad. Sci. U. S. A. 106*, 11028−11033.

(56) Swairjo, M. A., and Schimmel, P. R. (2005) Breaking sieve for steric exclusion of a noncognate amino acid from active site of a tRNA synthetase. *Proc. Natl. Acad. Sci. U. S. A. 102*, 988−993.

(57) Swairjo, M. A., Otero, F. J., Yang, X. L., Lovato, M. A., Skene, R. J., McRee, D. E., Ribas de Pouplana, L., and Schimmel, P. (2004) Alanyl-tRNA synthetase crystal structure and design for acceptor-stem recognition. *Mol. Cell 13*, 829−841.

(58) Guo, M., Shapiro, R., and Schimmel, P. a. Y., X.-L. (2010) Introduction of a leucine half-zipper engenders multiple high-quality crystals of a recalcitrant tRNA synthetase. *Acta Crystallogr., Sect. D D66*, 243−250.

(59) Ishijima, J., Uchida, Y., Kuroishi, C., Tuzuki, C., Takahashi, N., Okazaki, N., Yutani, K., and Miyano, M. (2006) Crystal structure of alanyl-tRNA synthetase editing-domain homolog (PH0574) from a hyperthermophile, Pyrococcus horikoshii OT3 at 1.45 Å resolution. *Proteins 62*, 1133−1137.

(60) Sokabe, M., Okada, A., Yao, M., Nakashima, T., and Tanaka, I. (2005) Molecular basis of alanine discrimination in editing site. *Proc. Natl. Acad. Sci. U. S. A. 102*, 11669−11674.

(61) Guo, M., Chong, Y. E., Shapiro, R., Beebe, K., Yang, X.-L., and Schimmel, P. (2009) Paradox of mistranslation of serine for alanine caused by AlaRS recognition dilemma. *Nature 462*, 808−812.

(62) Hill, K., and Schimmel, P. (1989) Evidence that the 3′ end of a tRNA binds to a site in the adenylate synthesis domain of an aminoacyl-tRNA synthetase. *Biochemistry 28*, 2577−2586.

(63) Francklyn, C. S. (2008) DNA polymerases and aminoacyl-tRNA synthetases: shared mechanisms for ensuring the fidelity of gene expression. *Biochemistry 47*, 11695−11703.

(64) Dock-Bregeon, A. C., Rees, B., Torres-Larios, A., Bey, G., Caillet, J., and Moras, D. (2004) Achieving error-free translation; the mechanism of proofreading of threonyl-tRNA synthetase at atomic resolution. *Mol. Cell 16*, 375−386.

(65) Putney, S. D., Sauer, R. T., and Schimmel, P. R. (1981) Purification and properties of alanine tRNA synthetase from Escherichia coli A tetramer of identical subunits. *J. Biol. Chem. 256*, 198−204.

(66) Laemmli, U. K. (1970) Cleavage of structural proteins during the assembly of the head of bacteriophage T4. *Nature 227*, 680−685.

(67) Dignam, J. D., Nada, S., and Chaires, J. B. (2003) Thermodynamic characterization of the binding of nucleotides to glycyl-tRNA synthetase. *Biochemistry 42*, 5333−5340.

(68) Dignam, S. S., and Dignam, J. D. (1984) Glycyl- and alanyl-tRNA synthetases from Bombyx mori. Purification and properties. *J. Biol. Chem. 259*, 4043−4048.

(69) Fromm, H. J. (1975) *Initial Rate Enzyme Kinetics*, Vol. *22*, pp 116−119, Springer-Verlag, New York.

(70) Jelesarov, I., and Bosshard, H. R. (1999) Isothermal titration calorimetry and differential scanning calorimetry as complementary tools to investigate the energetics of biomolecular recognition. *J. Mol. Recognit. 12*, 3−18.

(71) Hayes, D. B., Laue, T., and Philo, J. (2006) *Sedimentation Interpretation Program*, 1.09 ed., University of New Hampshire, Durham, NH.

(72) Yphantis, D., and Lary, J. W. (1999) WinMatch V0.99 for Win95 + WinNT, *Program for Intercomparison of Ultracentrifuge Data Files*, 0.99.0039 ed., Mansfield Center, CT.

(73) Schuck, P. (2008) SEDFIT, 11.3b ed., National Institutes of Health, Bethesda, MD.

(74) Schuck, P. (2000) Size-Distribution Analysis of Macromolecules by Sedimentation Velocity Ultracentrifugation and Lamm Equation Modeling. *Biophys. J. 78*, 1606−1619.

(75) Philo, J. S. (2007) DCDT+, 2.1.0.28333 ed., Thousand Oaks, CA.

(76) Philo, J. S. (2000) A Method for Directly Fitting the Time Derivative of Sedimentation Velocity Data and an Alternative Algorithm for Calculating Sedimentation Coefficient Distribution Functions. *Anal. Biochem. 279*, 151−163.

(77) Philo, J. (2006) Improved methods for fitting sedimentation coefficient distributions derived by time-derivative techniques. *Anal. Biochem. 354*, 238−246.

(78) Sherwood, P., and Stafford, W. (2008) SedAnal, sedimentation analysis software, 5.03 ed., Boston Biomedical Research Institute, Watertown, MA.

(79) Gillam, I. C., and Tenor, G. M. (1981) The use of BD-cellulose in separating transfer RNAs, in *RNA and Protein Synthesis, Selected Methods in Enzymology* (Colowick, S. P., and Kaplan, N. O., Eds.) pp 43−58, Academic Press, New York.

(80) Hauenstein, S. I., Hou, Y.-M., and Perona, J. J. (2008) The homotetrameric phosphoseryl-tRNA synthetase from Methanosarcina mazei exhibits half-of-the-sites activity. *J. Biol. Chem. 283*, 21997−22006.

(81) Guo, M., Ignatov, M., Musier-Forsyth, K., Schimmel, P., and Yang, X.-L. (2008) Crystal structure of tetrameric form of human lysyl-tRNA synthetase: Implications for multisynthetase complex formation. *Proc. Natl. Acad. Sci. U. S. A. 105*, 2331−2336.

(82) Beuning, P. J., and Musier-Forsyth, K. (1999) Transfer RNA recognition by aminoacyl-tRNA synthetases. *Biopolymers 52*, 1−28.

(83) O'Donoghue, P., Sethi, A., Woese, C. R., and Luthey-Schulten, Z. A. (2005) The evolutionary history of Cys-tRNACys formation. *Proc. Natl. Acad. Sci. U. S. A. 102*, 19003−19008.

(84) Ribas de Pouplana, L., and Schimmel, P. (1997) Reconstruction of quaternary structures of class II tRNA synthetases by rational mutagenensis of a conserved domain. *Biochemistry 36*, 15041−15048.

(85) Pasman, Z., Robey-Bond, S., Mirando, A. C., Smith, G. J., Lague, A., and Francklyn., C. S. (2011) Substrate Specificity and Catalysis by the Editing Active Site of Alanyl-tRNA Synthetase from *Escherichia coli*. *Biochemistry 50*, 1474−1482.

(86) Nass, G., and Stoffler, G. (1967) Molecular weight distribution of the aminoacyl-tRNA-synthetases of Escherichia coli by gel filtration. *Mol. Gen. Genet. 100*, 378−382.

(87) Filley, S. J., and Hill, K. A. (1993) Amino acid substitutions at position 73 in motif 2 of Escherichia coli alanyl-tRNA synthetase. *Arch. Biochem. Biophys. 307*, 46−51.

(88) Miller, W. T., Hill, K. A., and Schimmel, P. (1991) Evidence for a "cysteine-histidine box" metal-binding site in an Escherichia coli aminoacyl-tRNA synthetase. *Biochemistry 30*, 6970−6976.

(89) Wu, M. X., Filley, S. J., Xiong, J., Lee, J. J., and Hill, K. A. (1994) A cysteine in the C-terminal region of alanyl-tRNA synthetase is important for aminoacylation activity. *Biochemistry 33*, 12260−12266.

(90) Fromm, H. J. (1975) *Initial Rate Enzyme Kinetics*, Vol. *22*, pp 116−119, Springer-Verlag, New York.

(91) Ermolinsky, B. S., and Mikhailov, S. N. (2000) Periodate oxidation in chemistry of nucleic acids: dialdehyde derivitives of

nucleotides, nucleosides, and oligonucleosides (Review). *Russ. J. Bioorg. Chem. 26*, 429−449.
(92) Chou, C.-W., Limbach, P. A., and Cole, R. B. (2002) Fragmentation Pathway Studies of Oligonucleotides in Matrix-Assisted Laser Desorption/Ionization Mass Spectrometry by Charge Tagging and H/D Exchange. *J. Am. Soc. Mass Spectrom. 13*, 1407−1417.
(93) McLuckey, S. A., and Habibi-Goudarzi, S. (1993) Decompositions of Multiply Charged Oligonucleotide Anions. *J. Am. Chem. Soc. 115*, 12085−12095.
(94) Lechler, A., Martin, A., Zuleeg, T., Limmer, S., and Kreutzer, R. (1997) A biologically active 53 kDa fragment of overproduced alanyl-tRNA synthetase from Thermus thermophilus HB8 specifically interacts with tRNA Ala acceptor helix. *Nucleic Acids Res. 25*, 2737−2744.
(95) Nishio, K., and Kawakami, M. (1984) Two-domain structure of alanyl-tRNA synthetase from Bombyx mori: isolation of the N-terminal catalytic domain. *J. Biochem. (Tokyo) 96*, 1875−1881.
(96) Nishio, K., and Kawakami, M. (1984) Purification and properties of alanyl-tRNA synthetase from Bombyx mori: a monomeric enzyme. *J. Biochem. (Tokyo) 96*, 1867−1874.
(97) Shiba, K., Ripmaster, T., Suzuki, N., Nichols, R., Plotz, P., Noda, T., and Schimmel, P. (1995) Human alanyl-tRNA synthetase: conservation in evolution of catalytic core and microhelix recognition. *Biochemistry 34*, 10340−10349.
(98) Jasin, M., Regan, L., and Schimmel, P. (1985) Two mutations in the dispensable part of alanine tRNA synthetase which affect the catalytic activity. *J. Biol. Chem. 260*, 2226−2230.
(99) Spolar, R. S., and Record, M. T. (1994) Coupling of local folding to site specific binding of proteins to DNA. *Science 263*, 777−784.
(100) Sankaranarayanan, R., Dock-Bregeon, A. C., Romby, P., Caillet, J., Springer, M., Rees, B., Ehresmann, C., Ehresmann, B., and Moras, D. (1999) The structure of threonyl-tRNA synthetase-tRNA(Thr) complex enlightens its repressor activity and reveals an essential zinc ion in the active site. *Cell 97*, 371−381.